Electronic Supplementary Material (ESI) for Journal of Materials Chemistry A.

Supplementary Information

Light-induced reactivity of gold and hybrid perovskite as a new possible degradation mechanism in perovskite solar cells

Natalia N. Shlenskaya[a], Nikolai A. Belich[a], Michael Graetzel[b], Eugene A. Goodilin[a,c], Alexey B. Tarasov[a,c]**

[a] Laboratory of New Materials for Solar Energetics, Department of Materials Science, Lomonosov Moscow State University, Lenin Hills, 119991, Moscow, Russia

[b] Laboratory of Photonics and Interfaces, Institute of Chemical Sciences and Engineering École Polytechnique Fédérale de Lausanne (EPFL), Station 6, CH-1015 Lausanne, Switzerland

[c] Laboratory of Inorganic Materials, Department of Chemistry, Lomonosov Moscow State University, Lenin Hills, 119991, Moscow, Russia

* Corresponding authors

Content

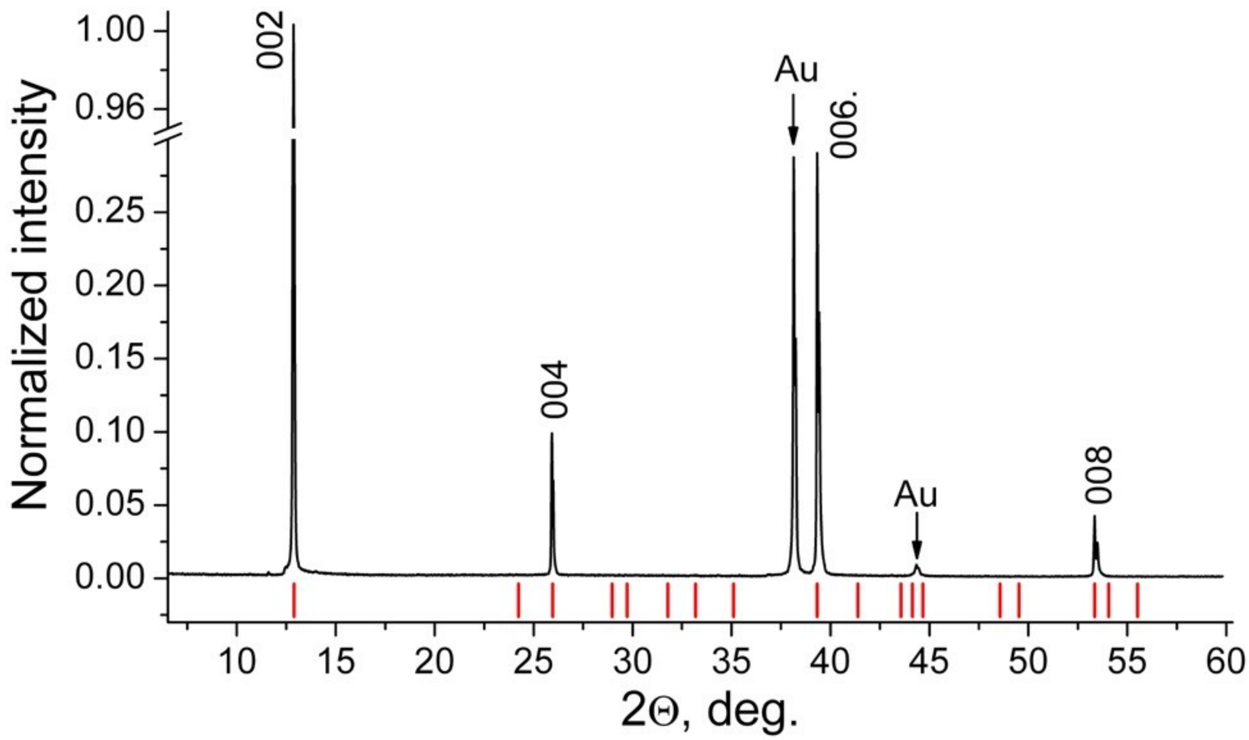

Figure S1. XRD pattern of gold after interaction with melted iodine at 170^{o}C. Red bars correspond to AuI reflections (JCPDS card no. 15-521).

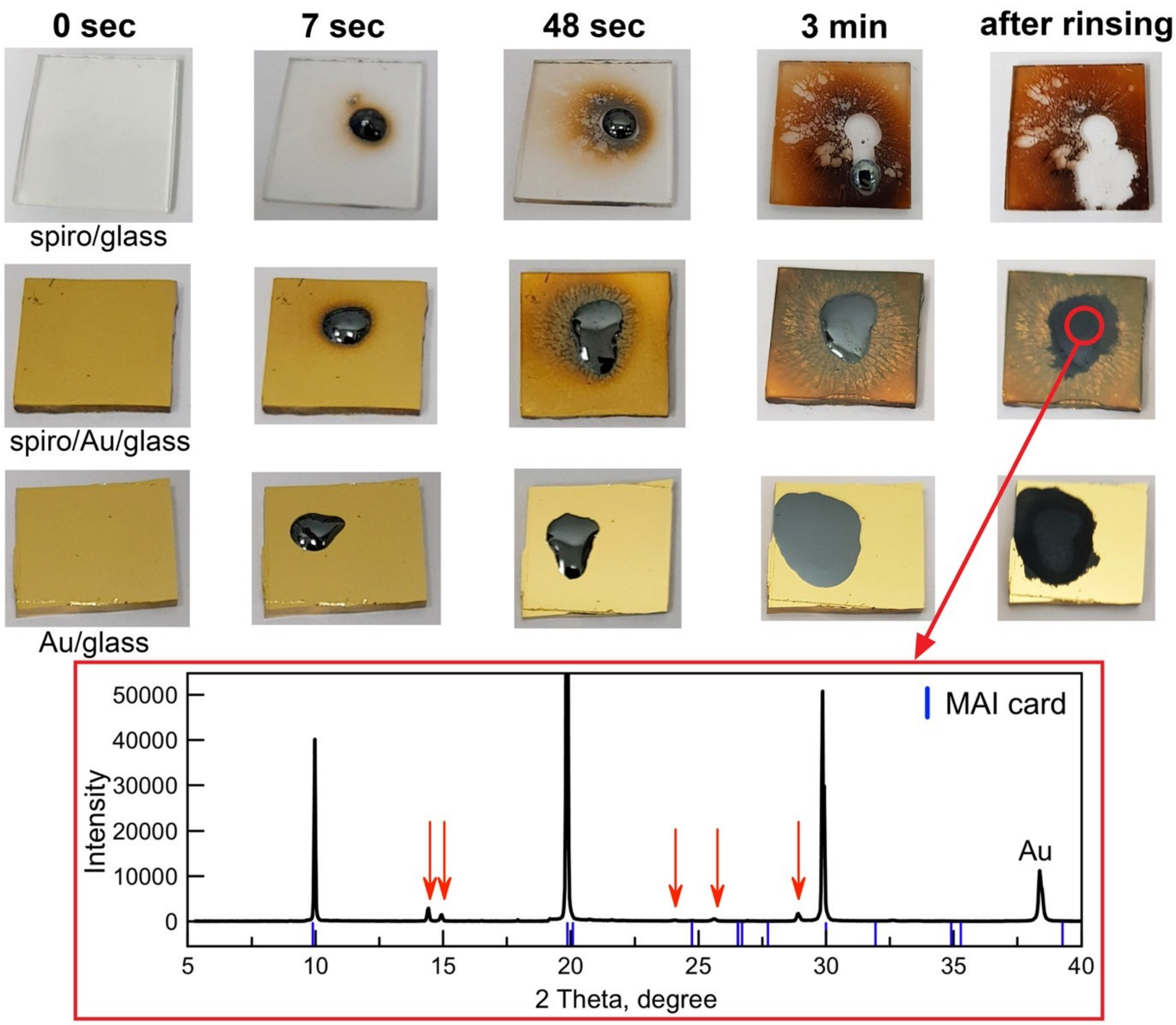

Figure S2. Chemical interaction between RPMs and thin films of spiro-OMeTAD (top), spiro-OMeTAD/gold (middle), and gold (bottom). Inset shows XRD pattern of the black film formed after 3 min interaction between RPMs and spiro-OMeTAD/Au film and rinsing it in CCl_4. Red arrows indicate reflections of the "black phase", other reflections correspond to MAI and metallic gold.

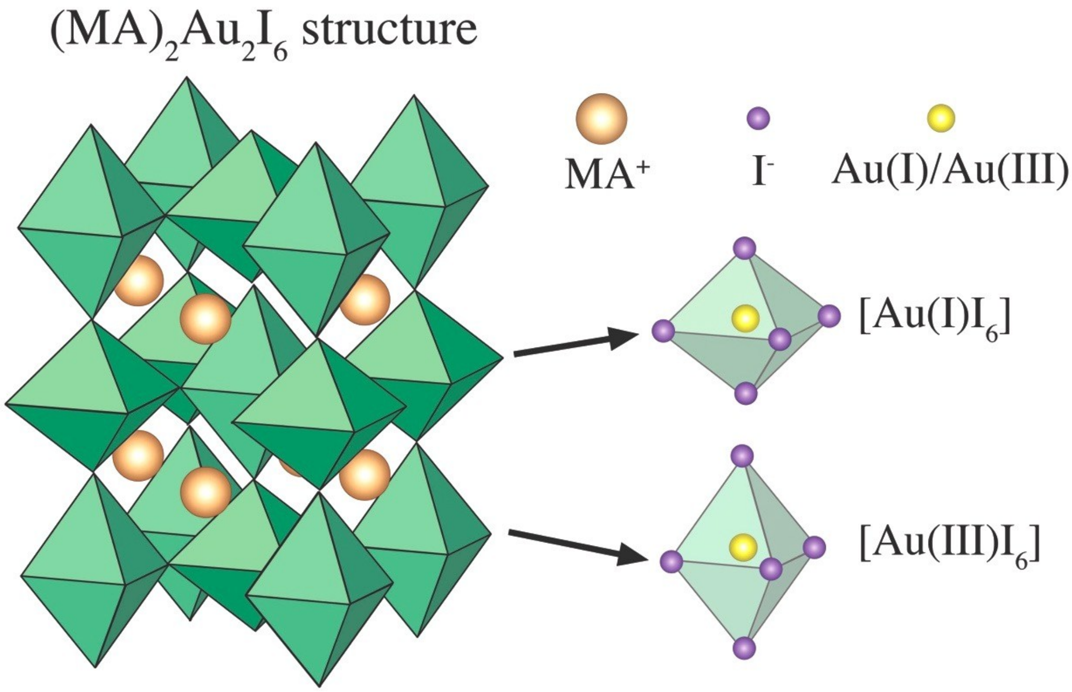

Figure S3. Crystal structure of $(MA)_2Au_2I_6$ which consists of compressed $Au(I)I_6$ and elongated $Au(III)I_6$ octahedra, revealing the distorted tetragonal perovskite structure

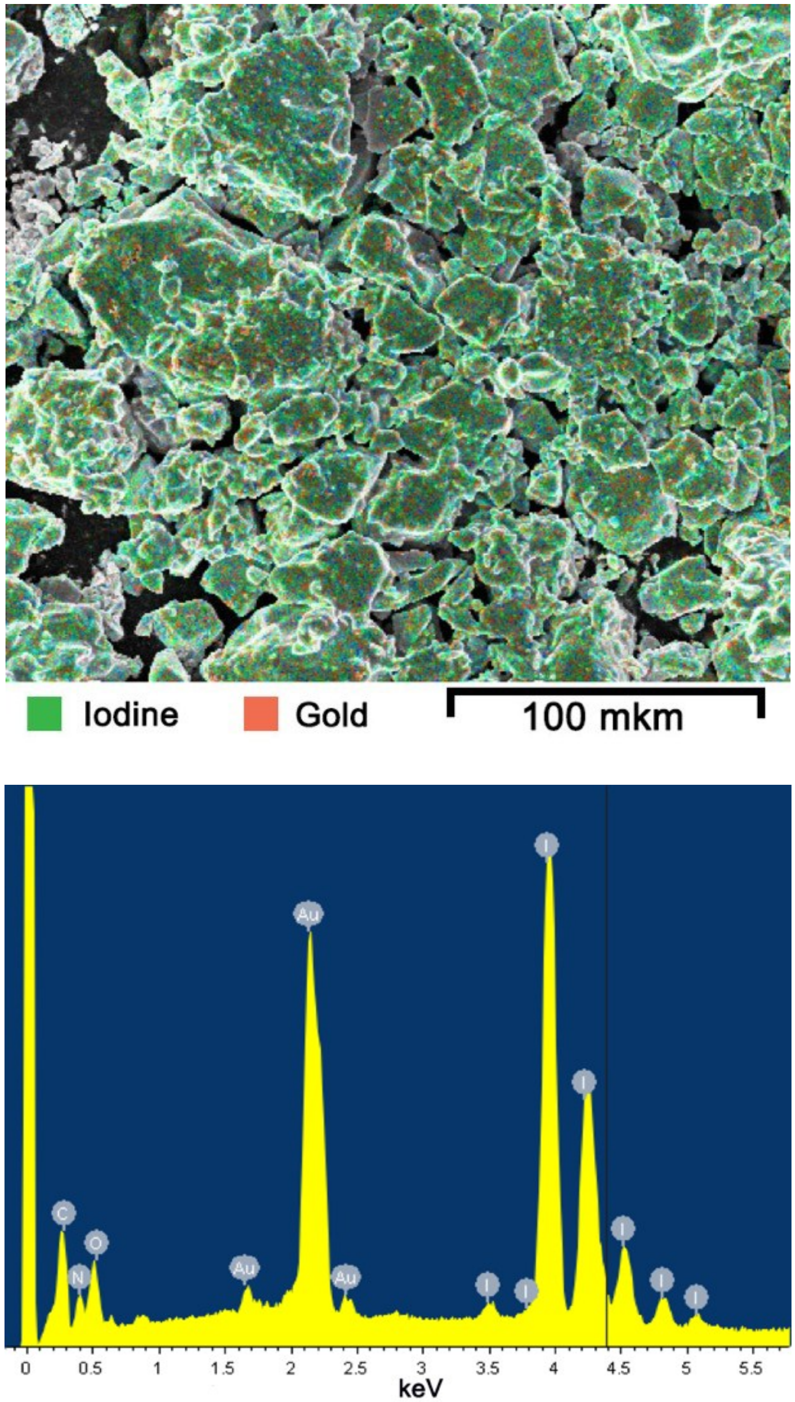

Figure S4. Elemental mapping of the single-phase $(MA)_2Au_2I_6$ sample in SEM (top) and corresponding to this map X-ray energy-dispersive spectrum (bottom).

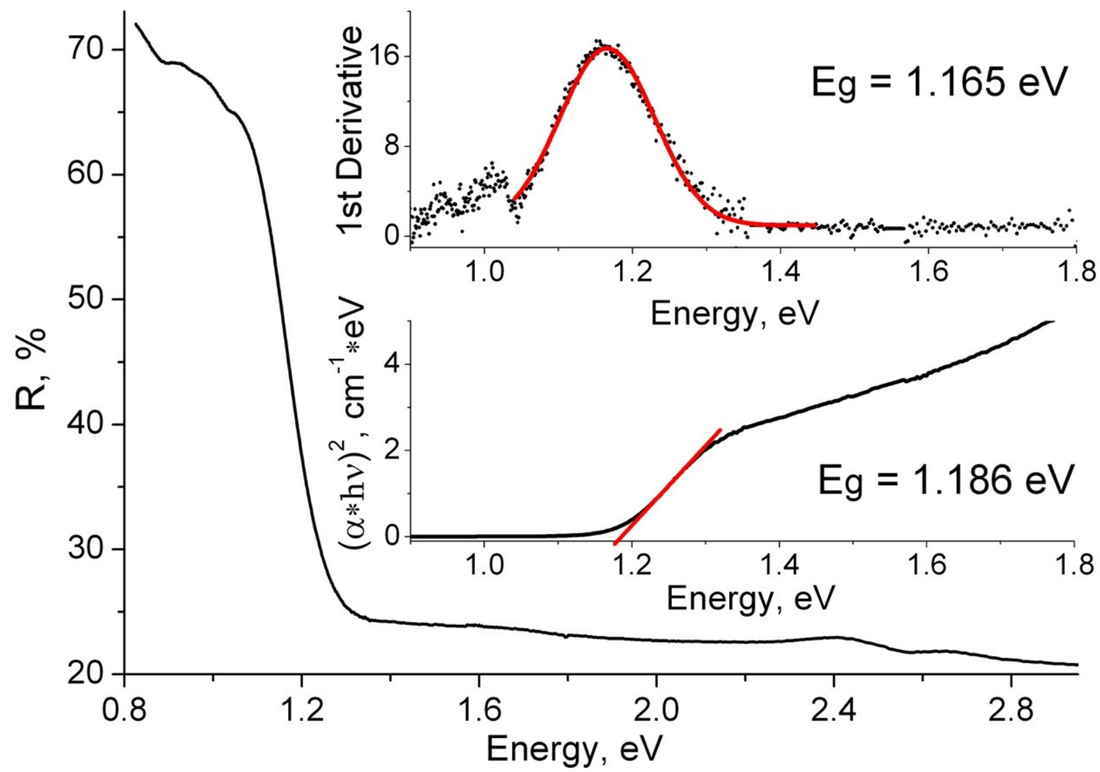

Figure S5. Diffuse reflectance spectrum of $(MA)_2Au_2I_6$ phase and the corresponding bandgap energy analysis via first derivative method (top inset) and Kubelka-Munk function (bottom inset).

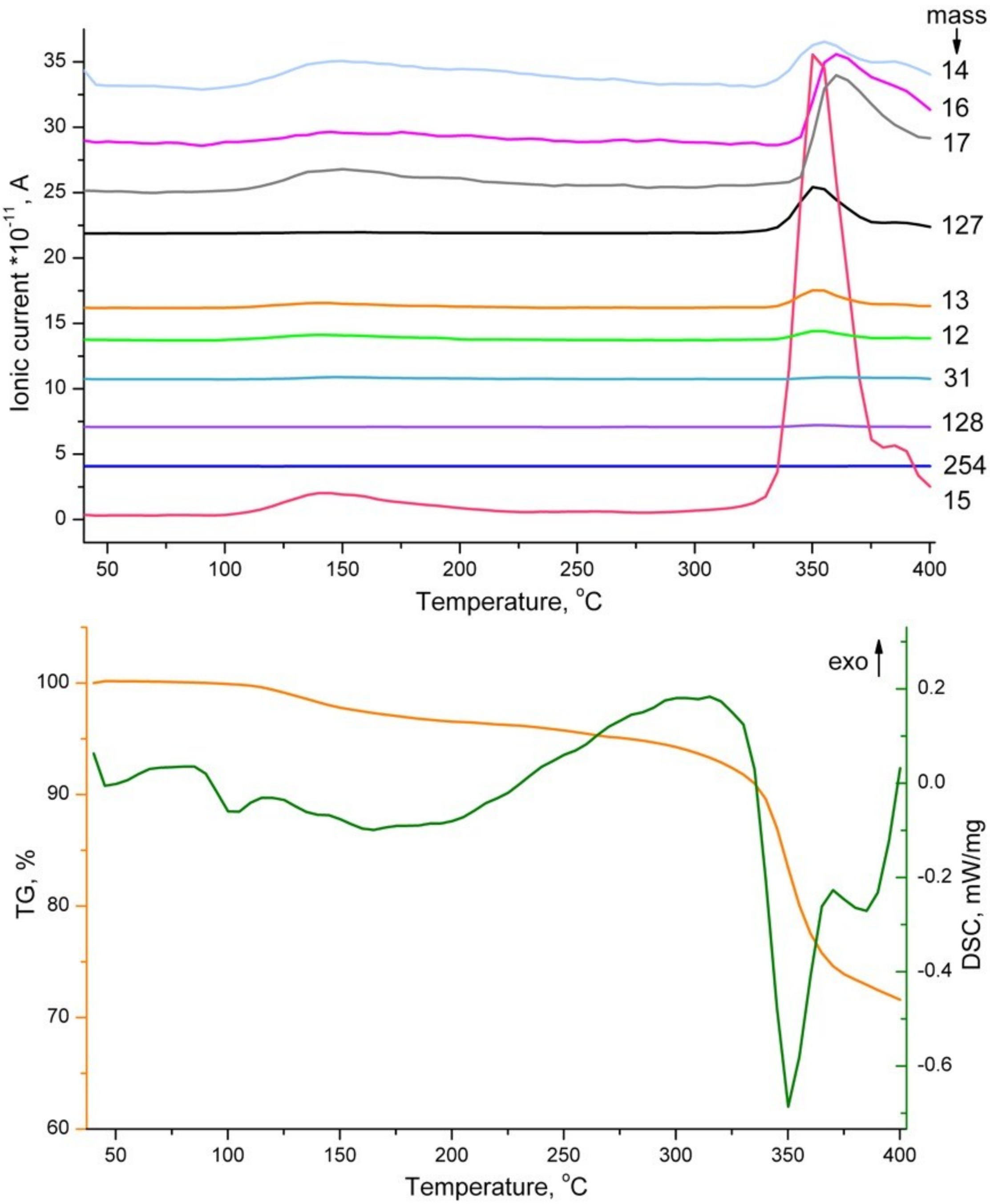

Figure S6. Thermogravimetric analysis of MAPI including particles masses (top); differential scanning calorimetry of MAPI (bottom).

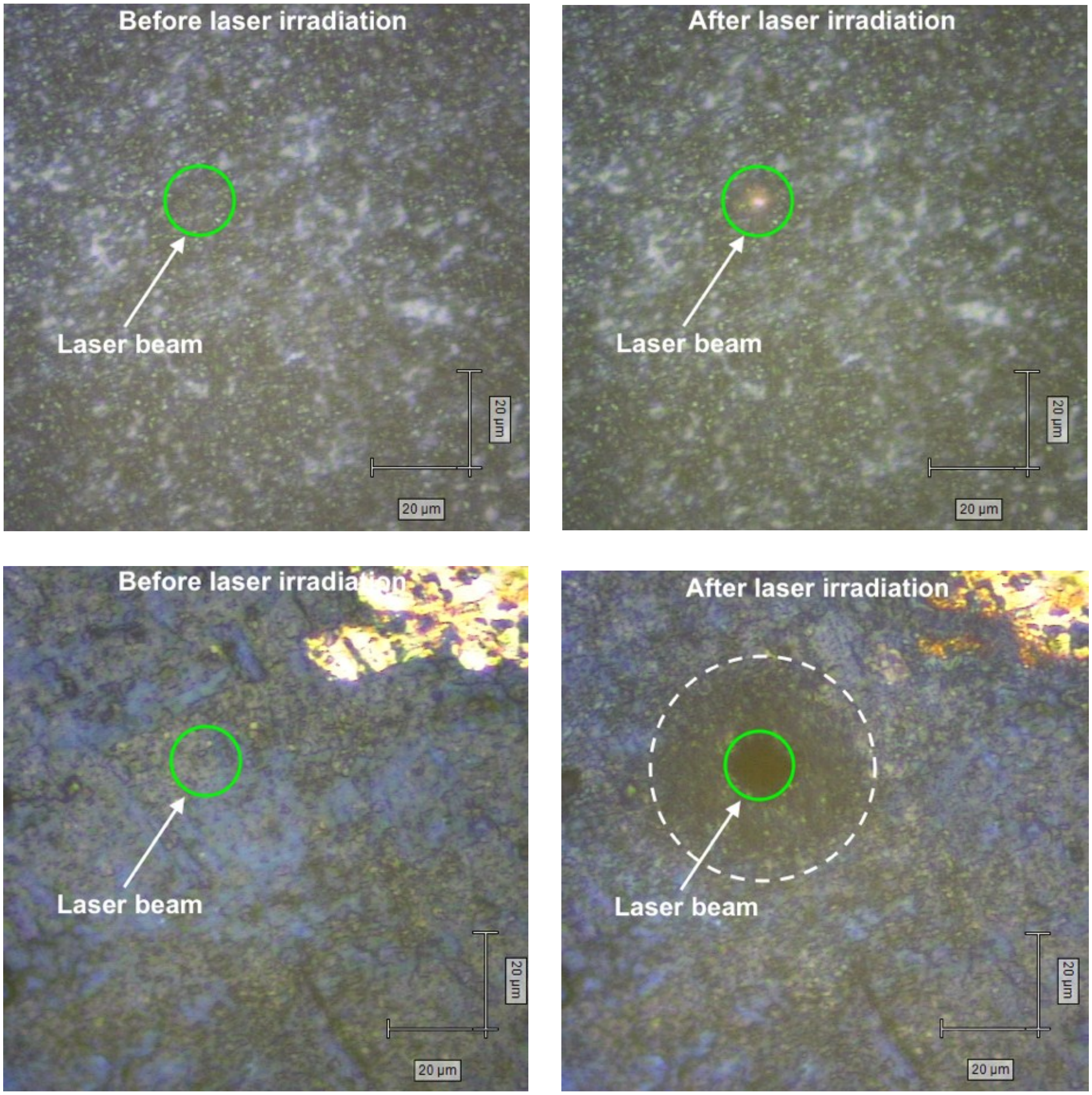

Figure S7. Optical photographs of $(MA)_2Au_2I_6$ sample before (left) and after (right) laser beam irradiation in Raman spectrometer. Excitation wavelength is 514 nm.

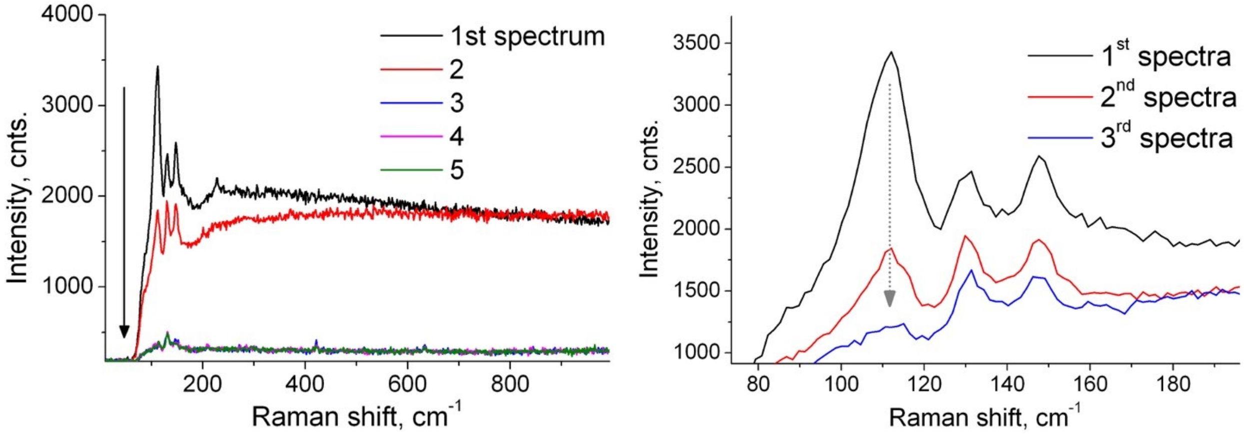

Figure S8. Evolution of Raman spectra during repeated laser irradiation, showing rapid degradation of $(MA)_2Au_2I_6$ sample under laser beam.

$(MA)_2Au_2I_6$ undergoes rapid degradation under the 514 nm laser beam with relatively high intensity which explains some discrepancies reported for similar complex iodides in the literature.[1,2] Degradation is accompanied with the release of iodine and metallic gold as clearly seen in the view field of an optical microscope (see Figure S6) and is confirmed by the temporal evolution of Raman spectra in the series of consequential measurements (see Figure S7).

(1) Wang, S.; Kemper, A. F.; Baldini, M.; Shapiro, M. C.; Riggs, S. C.; Zhao, Z.; Liu, Z.; Devereaux, T. P.; Geballe, T. H.; Fisher, I. R.; *et al.* Bandgap Closure and Reopening in CsAuI3 at High Pressure. *Phys. Rev. B - Condens. Matter Mater. Phys.* **2014**, *89*, 1–7.

(2) Gheorghe, D.-E. Solid State Chemistry of Mixed-Valent Gold(I/III) Bromides, 2008.

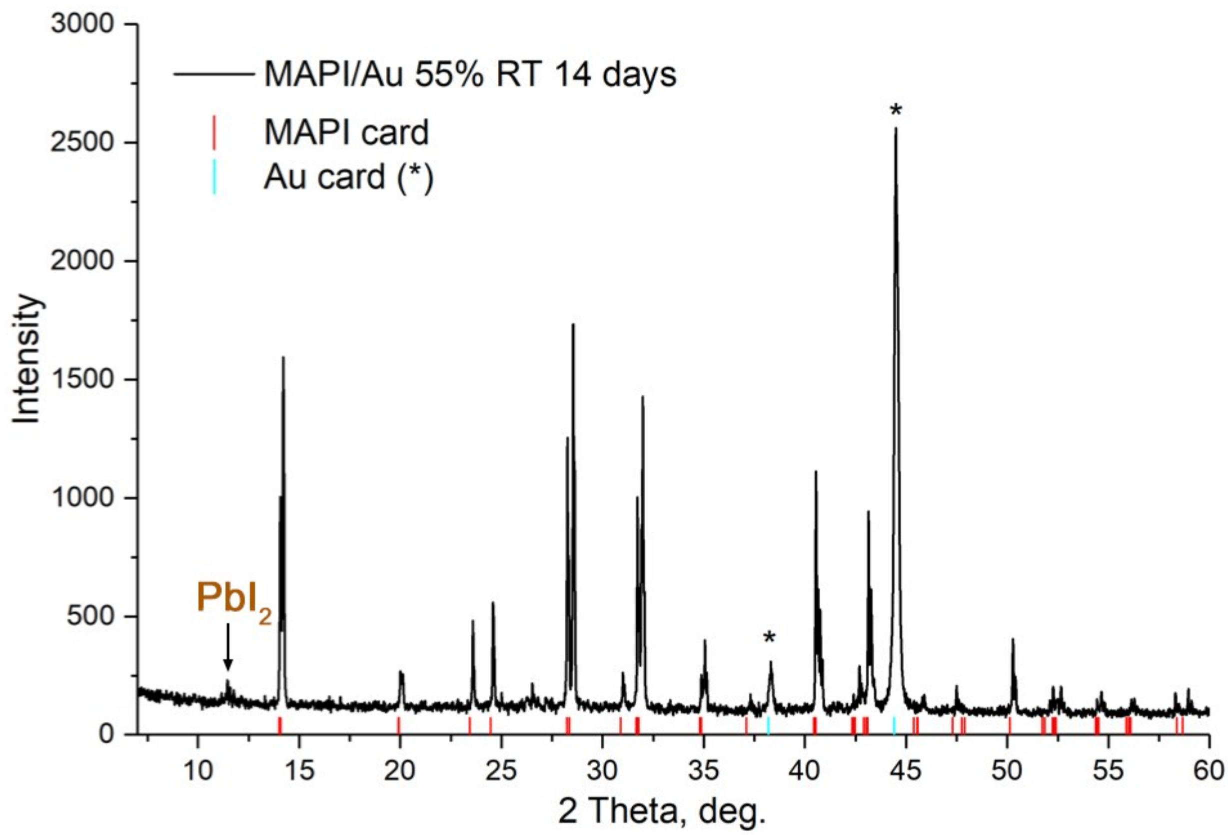

Figure S9. The absence of gold transformation into complex phases in the experiment on degradation of the MAPI/Au powders mixture under 55% relative humidity for 14 days in a desiccator.